Study of Morphology and Phase Diagram of π-Shaped ABC Block Copolymers Using Self-Consistent-Field Theory

Xianggui Ye,[†] Tongfei Shi,[†] Zhongyuan Lu,[‡] Chengxiang Zhang,[§] Zhaoyan Sun,*,[†] and Lijia An*,[†]

State Key Laboratory of Polymer Physics and Chemistry, Changchun Institute of Applied Chemistry, Chinese Academy of Sciences, Changchun, 130022, P. R. China; State Key Laboratory of Computational and Theoretical Chemistry, Jilin University, Changchun, 130023, P. R. China; and Department of Physics, Jilin University, Changchun, 130023, P. R. China

ABSTRACT: Using a combinatorial screening method based on the self-consistent-field theory for polymers, we study the bulk morphology and the phase behavior of π-shaped ABC block copolymers, in which A is the backbone and B and C are the two grafts. By systematically varying the positions of the graft points, the π-shaped block copolymer can change from a star block copolymer to a linear ABC block copolymer. Thus, the corresponding order−order phase transition due to the architecture variation can be investigated. At two given compositions, we find seven different morphologies ("three-color" lamellar phase, "three-color" hexagonal honeycomb phase, lamellae with beads inside, dodecagon−hexagon−tetragon, hexagon−hexagon, lamellae with alternating beads, and octagon−octagon−tetragon). The hexagon−hexagon morphology has not been reported previously for linear and star triblock copolymers in the bulk state. The phase diagram of the π-shaped ABC block copolymer with symmetric interactions among the three species is constructed. When the volume fractions of block B and block C are equal, the triangle phase diagram shows reflection symmetry. When the shorter block is fixed at the backbone end and the other block moves to the other end along the backbone, the resulting morphology reaches to the same as that of a linear triblock copolymer rapidly. These results may help the design of the microstructures of complex block copolymers.

Introduction

As a fertile source of soft materials, block copolymers have attracted a great deal of attention among both academic and industrial researchers. A lot of work has been devoted to studies on block copolymers of different architectures because they may self-organize and undergo phase separation, leading to various morphologies and interesting properties. It has been demonstrated both theoretically and experimentally that the architecture of block copolymers is an important controlling factor for their morphological behavior.[1−6] Graft or star block copolymers are able to yield morphologies that are not available to corresponding linear block copolymers of the same composition and interaction energies.[7] Recently, Tang et al. systematically investigated the morphology of linear ABC block copolymer and star ABC block copolymer via the self-consistent-field theory (SCFT); they found that at the same composition and interaction energies a linear ABC triblock copolymer and a star ABC block copolymer exhibit different morphologies.[8,9]

A π-shaped ABC block copolymer molecule has two graft points. By changing the positions of the graft points, one can obtain block copolymers of different architectures. When the two grafts connect to the backbone at two positions other than the end points, the copolymer molecule is π-shaped. If the two graft points are at different ends of the backbone, the π-shaped block copolymer turns into a linear triblock copolymer. If the two graft points are at the same position, the π-shaped block copolymer then becomes a star block copolymer. Because a π-shaped block copolymer can evolve into copolymers of various architectures, leading to rich morphologies, it becomes a good model for studying the order−order transition.

Experimentally, π-shaped double-graft copolymers and H-shaped double-graft copolymers have been synthesized by Lee et al. via anionic polymerization.[3,4] In their studies, it was concluded that the effect of bridge connections on the morphology of the copolymer is close to negligible when the molecular weight is high. Thus, they can estimate the morphological behavior of molecular of architectures with multiple junction points by imagining all bridge and loop blocks to be cut in half. However, the effect of bridge connections on morphology cannot be neglected for copolymers of low or intermediate molecular weight. Therefore, it is necessary to study, in this regime, the morphology transition of the π-shaped block copolymer by systematically changing the positions of the two grafts, i.e., the bridge length of the block copolymer.

The self-consistent-field theory is accurate and suitable to investigate and screen the microphase separation behavior. Earlier applications of self-consistent mean-field theory (SCMFT) to diblock and triblock copolymers were introduced by Helfand et al.[10−12] and by Noolandi et al.[13−15] They established phase diagrams of AB diblock and ABA triblock copolymers in the parameter space of the "incompatibility degree" $\chi_{AB}N$ and composition f_A. In recent years, Matsen and Schick proposed a powerful numerical spectral method that could be used to deal with microphases of considerable

[†] Chinese Academy of Sciences.
[‡] State Key Laboratory of Computational and Theoretical Chemistry, Jilin University.
[§] Department of Physics, Jilin University.
* Corresponding authors: e-mail zysun@ciac.jl.cn or ljan@ciac.jl.cn; Tel +86-431-5262137 or +86-431-5262206; Fax +86-431-5262969 or +86-431-5685653.

three-dimensional complexity.[16−19] This method is accurate enough but requests a prior knowledge of the symmetry of the ordered structure, which has hindered its application in finding previously unknown microphases of complex copolymer structures. More recently, Drolet and Fredrickson suggested a new combinatorial screening method,[20−22] which involves a direct implementation of SCFT in real space in an adaptive arbitrary cell. This method proves to be very successful and can be applied to complex copolymer melts.

In this work, we use the combinatorial screening method to study the equilibrium morphologies of π-shaped ABC block copolymers. Moreover, the order−order transitions due to changing the positions of the graft points (i.e., from linear triblock copolymer to star block copolymer) at a given composition are investigated.

Theoretical Method

A schematic representation of the architecture of the π-shaped ABC block copolymer is shown in Figure 1. The total degree of polymerization of the π-shaped block copolymer is N, and the A, B, and C blocks consist of $f_A N$, $f_B N$, and $f_C N$ monomers, respectively. Two graft points divide the block copolymer into five parts, namely A1, A2, A3, B, and C as shown in Figure 1. The polymer segment probability distribution function $q_{\alpha\beta}(\mathbf{r},s)$, representing the probability of finding segment s at position $\mathbf{r}$, satisfies the modified diffusion equation (eq 1) with $\alpha = A1, A2, A3, B, C$ and $\beta = 0, 1$. $\beta = 0$ corresponds to s of $q_{\alpha\beta}(\mathbf{r},s)$ increasing from the free end to the near graft point or from graft point B to C, and $\beta = 1$ corresponds to s of $q_{\alpha\beta}(\mathbf{r},s)$ increasing from the near graft point to the free end or from graft point C to B.

The modified diffusion equation reads

$$\frac{\partial q_{\alpha\beta}(\mathbf{r},s)}{\partial s} = \nabla^2 q_{\alpha\beta}(\mathbf{r},s) - W_\alpha(\mathbf{r})\, q_{\alpha\beta}(\mathbf{r},s) \quad (1)$$

where $W_\alpha(\mathbf{r})$ is the self-consistent field for species α, and $0 < s < f_\alpha N$. The initial conditions of $q_{\alpha\beta}(\mathbf{r},s)$ are

$$q_{A10}(\mathbf{r},0) = q_{A30}(\mathbf{r},0) = q_{B0}(\mathbf{r},0) = q_{C0}(\mathbf{r},0) = 1.0$$

$$q_{A20}(\mathbf{r},0) = q_{A10}(\mathbf{r},f_{A1}N)\, q_{B0}(\mathbf{r},f_B N)$$

$$q_{A11}(\mathbf{r},0) = q_{A21}(\mathbf{r},f_{A2}N)\, q_{B0}(\mathbf{r},f_B N)$$

$$q_{A21}(\mathbf{r},0) = q_{A30}(\mathbf{r},f_{A3}N)\, q_{C0}(\mathbf{r},f_C N)$$

$$q_{A31}(\mathbf{r},0) = q_{A20}(\mathbf{r},f_{A2}N)\, q_{C0}(\mathbf{r},f_C N)$$

$$q_{B1}(\mathbf{r},0) = q_{A10}(\mathbf{r},f_{A1}N)\, q_{A21}(\mathbf{r},f_{A2}N)$$

$$q_{C1}(\mathbf{r},0) = q_{A20}(\mathbf{r},f_{A2}N)\, q_{A30}(\mathbf{r},f_{A3}N)$$

which are similar to those in ref 9. The partition function of a single chain subject to the self-consistent-field $W_\alpha(\mathbf{r})$ can be written as $Q = \int d\mathbf{r}\, q_{\alpha0}(\mathbf{r},s)\, q_{\alpha1}(\mathbf{r},f_\alpha N - s)$, whose derivation of the single-chain partition function is the same as that of the star triblock copolymer.[9] It should be noted that Q is independent of the chain contour length parameter s.
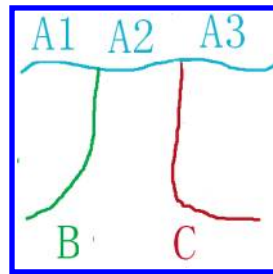

Figure 1. Molecular architecture of the π-shaped ABC block copolymer.

With the above description, the free energy of the system is given by

$$\frac{F}{nk_B T} = -\ln\!\left(\frac{Q}{V}\right) + \frac{1}{V}\int d\mathbf{r}\, [\chi_{AB}N(\phi_A(\mathbf{r}) - f_A)(\phi_B(\mathbf{r}) -$$
$$f_B) + \chi_{BC}N(\phi_B(\mathbf{r}) - f_B)(\phi_C(\mathbf{r}) - f_C) + \chi_{AC}N(\phi_A(\mathbf{r}) -$$
$$f_A)(\phi_C(\mathbf{r}) - f_C) - W_A(\mathbf{r})(\phi_A(\mathbf{r}) - f_A) - W_B(\mathbf{r})(\phi_B(\mathbf{r}) -$$
$$f_B) - W_C(\mathbf{r})(\phi_C(\mathbf{r}) - f_C) - P(\mathbf{r})(1 - \phi_A(\mathbf{r}) - \phi_B(\mathbf{r}) -$$
$$\phi_C(\mathbf{r}))] \quad (2)$$

where V is the volume of the system; ϕ_A, ϕ_B, and ϕ_C are the monomer density fields normalized by the local volume fractions of A, B, and C, respectively; χ_{AB}, χ_{BC}, and χ_{AC} are Flory−Huggins parameters between different species; $P(\mathbf{r})$ is the potential field that ensures the incompressibility of the system. Minimizing the free energy with respect to ϕ_A, ϕ_B, ϕ_C, W_A, W_B, W_C, and $P(\mathbf{r})$ leads to the following self-consistent-field equations that describe the equilibrium morphology:

$$W_A(\mathbf{r}) = \chi_{AB}N(\phi_B(\mathbf{r}) - f_B) + \chi_{AC}N(\phi_C(\mathbf{r}) - f_C) + P(\mathbf{r}) \quad (3)$$

$$W_B(\mathbf{r}) = \chi_{AB}N(\phi_A(\mathbf{r}) - f_A) + \chi_{BC}N(\phi_C(\mathbf{r}) - f_C) + P(\mathbf{r}) \quad (4)$$

$$W_C(\mathbf{r}) = \chi_{AC}N(\phi_A(\mathbf{r}) - f_A) + \chi_{BC}N(\phi_B(\mathbf{r}) - f_B) + P(\mathbf{r}) \quad (5)$$

$$\phi_A + \phi_B + \phi_C = 1 \quad (6)$$

$$\phi_A(\mathbf{r}) = \frac{V}{NQ}\int_0^{f_{A1}N} ds\, q_{A10}(\mathbf{r},s)\, q_{A11}(\mathbf{r},f_{A1}N - s) +$$
$$\frac{V}{NQ}\int_0^{f_{A2}N} ds\, q_{A20}(\mathbf{r},s)\, q_{A21}(\mathbf{r},f_{A2}N - s) +$$
$$\frac{V}{NQ}\int_0^{f_{A3}N} ds\, q_{A30}(\mathbf{r},s)\, q_{A31}(\mathbf{r},f_{A3}N - s) \quad (7)$$

$$\phi_B(\mathbf{r}) = \frac{V}{NQ}\int_0^{f_B N} ds\, q_{B0}(\mathbf{r},s)\, q_{B1}(\mathbf{r},f_B N - s) \quad (8)$$

$$\phi_C(\mathbf{r}) = \frac{V}{NQ}\int_0^{f_C N} ds\, q_{C0}(\mathbf{r},s)\, q_{C1}(\mathbf{r},f_C N - s) \quad (9)$$

The pressure field can be obtained by solving eqs 3−6:[23]

$$P = (C_2 C_3 (W_A + W_B) + C_1 C_3 (W_B + W_C) + C_1 C_2 (W_A + W_C))/2(C_1 C_2 + C_2 C_3 + C_1 C_3) \quad (10)$$

where

$$C_1 = -\chi_{AB}N + \chi_{BC}N + \chi_{AC}N \qquad (11)$$

$$C_2 = \chi_{AB}N - \chi_{BC}N + \chi_{AC}N \qquad (12)$$

$$C_3 = \chi_{AB}N + \chi_{BC}N - \chi_{AC}N \qquad (13)$$

The density field ϕ_α of species α conjugated to the self-consistent-field $W_\alpha(\mathbf{r})$ can be updated by using the equation[23]

$$W_\alpha^{\text{new}} = W_\alpha^{\text{old}} + \Delta t \left(\frac{\delta F}{\delta \phi_\alpha} \right)^* \qquad (14)$$

where the time step $\Delta t = 0.1$ and

$$\left(\frac{\delta F}{\delta \phi_\alpha} \right)^* = \sum_{M \neq \alpha} \chi_{\alpha M} N (\phi_M - f_M) + P(\mathbf{r}) - W_\alpha^{\text{old}} \qquad (15)$$

The initial value of $W_\alpha(\mathbf{r})$ is constructed by $W_\alpha(\mathbf{r}) = \sum_{M \neq \alpha} \chi_{\alpha M} N (\phi_M(\mathbf{r}) - f_M)$, where $\phi_M(\mathbf{r}) - f_M$ satisfies the Gaussian distribution:

$$\langle (\phi_M - f_M) \rangle = 0 \qquad (16)$$

$$\langle (\phi_i(r) - f_i)(\phi_j(r') - f_j) \rangle = \gamma f_i f_j \delta_{ij} \delta(r - r') \qquad (17)$$

Here γ is defined as the density fluctuation at the initial temperature. The above steps are iterated until the free energy converges to a local minimum, where the phase structure corresponds to a metastable or stable state. Each minimization is run several times using different initial random guess of the self-consistent fields $W_\alpha(\mathbf{r})$. In constructing the phase diagrams, we have encountered metastable structures. In each of these cases, we have identified the most stable structure by comparing the free energies.

For the sake of numerical tractability, the implementation of the self-consistent-field equations is carried out in a two-dimensional square grid with side length $L = V^{1/2}$, which is initially chosen to be a small value and is then increased until the changes in free energy are below some threshold.[20] The boundary conditions are periodic. The chain length of the polymers is fixed to be $N = 100$.

Results and Discussion

Tang et al. have mentioned that at the same composition and interactions ABC linear triblock copolymers and ABC star triblock copolymers have different phase diagrams.[8,9] However, when one of the blocks is relatively short, the influence of the star architecture on the morphology is not significant.[8,9] In this work we investigate the equilibrium morphologies of π-shaped ABC block copolymers with symmetric grafting $f_B = f_C = 0.3$ and asymmetric grafting $f_B = 0.2$ and $f_C = 0.4$. The interactions between the species are set to be the same, i.e., $\chi_{AC}N = \chi_{BC}N = \chi_{AB}N = 50$. Thus, there are only two variable parameters f_{A1} and f_{A2}. By changing the values of f_{A1} and f_{A2}, a triangle phase diagram corresponding to different positions of the graft points is constructed, and the influence of the graft points can be investigated. In the phase diagram (see Figure 2), the increment of f_{A1}/f_A, f_{A2}/f_A, and f_{A3}/f_A is 0.10. At $f_{A1}/f_A = 1.0$ (point **O**) and $f_{A3}/f_A = 1.0$ (point **Q**) in the phase diagram, the π-shaped ABC block copolymer becomes
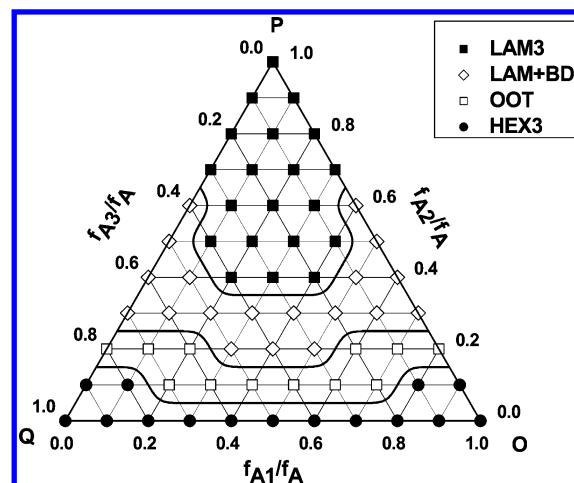

Figure 2. Phase diagram for $f_A = 0.40$, $f_B = f_C = 0.30$, and $\chi_{AB}N = \chi_{AC}N = \chi_{BC}N = 50$. The solid lines are shown to guide the eye.

an ABC star triblock copolymer. At $f_{A2}/f_A = 1.0$ (point **P**), the π-shaped ABC block copolymer becomes a linear BAC triblock copolymer. At each grid point, the morphology is obtained with the method described in the Theoretical Method section. Table 1 shows all microphases which are found for π-shaped ABC block copolymers. Three different colors, blue, green, and red, are assigned to A, B, and C blocks, respectively.

A. Two Grafts with Equal Lengths ($f_B = f_C = 0.30$). To focus on the influence of the graft point position on the phase behavior, first we study the order−order transition from the ABC star block copolymer to BAC linear block copolymer with the length of the B and C grafts being equal ($f_A = 0.40$, $f_B = f_C = 0.30$).
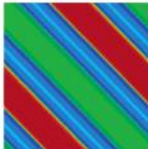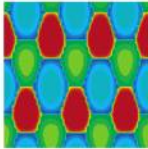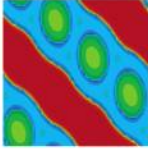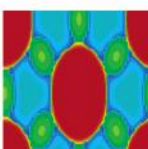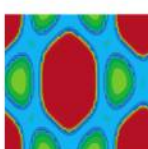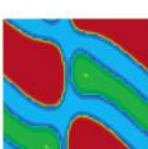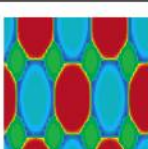
In Figure 2, the triangle phase diagram clearly shows a reflection symmetry with respect to the vertical line where $f_{A1}/f_A = 0.50$. Exchanging the positions of B and C graft points does not alter this symmetry for systems with equal interactions between the three distinct blocks. This feature arises from the particular molecular architecture of the π-shaped block copolymers with $f_B = f_C$. However, the reflection symmetry will vanish when $f_B \neq f_C$, which will be discussed later.

At the **OP** edge, $f_{A3}/f_A = 0.0$, which corresponds to fixing the C graft point at one end of the backbone A. Increasing f_{A2}/f_A corresponds to moving the B graft point to the other end of the backbone A. Accordingly, the ordered microphases change from HEX3, to LAM + BD, and finally to LAM3.

At the **OQ** edge of the triangle phase diagram in Figure 2, the volume fraction of A2 is zero and the π-shaped block copolymer becomes a star block copolymer. The architecture of the molecule changes from three-arm to four-arm and finally to three-arm again along the **OQ** edge, yet only one morphology (HEX3) is found, which is the same as that reported in the ref 9, where HEX3 is found at $f_A = 0.4$, $f_B = f_C = 0.3$ with $\chi_{AC}N = \chi_{BC}N = \chi_{AB}N = 35$. This shows that changing the number of arms in the present star block copolymer does not alter the HEX3 morphology.

Near the **OQ** edge, for example when $f_{A2}/f_A = 0.1$ (i.e., the volume fraction of A2 is 0.04), the OOT morphology is found. Different types of microphases appear with increasing f_{A2}/f_A. When f_{A2}/f_A is large enough, only one type of microphase (LAM3) is observed. These phenomena should arise from the particular characteristics of the π-shaped block copolymers. The A2 block joins block

Table 1. Summary of Observed Equilibrium Morphologies

Name	Abbreviation	Graphic
"three-color" lamellar phase	LAM3	
"three-color" hexagonal honeycomb phase	HEX3	
lamellae with beads inside	LAM +BD-I	
dodecagon-hexagon-tetragon	DOHT	
hexagon-hexagon	HEX2	
lamellae with alternating beads	LAM +BD	
octagon-octagon-tetragon	OOT	

B and block C, and the two graft points can be regarded as one when f_{A2}/f_A is small. In other words, the π-shaped block copolymer is similar to a four-arm star block copolymer when f_{A2}/f_A is very small. When f_{A2}/f_A is large enough, however, the distance between the two graft points is very large, and the π-shaped block copolymer is similar to a linear triblock copolymer. We should also note that the morphology changes are very small along the **OQ** direction, compared to that along the **OP** direction. Along the **OQ** direction, the copolymer molecule maintains its π-shaped architecture, and only the lengths of the two dangling backbone blocks (A1 and A3) change; i.e., the architecture does not change much. On the other hand, along the **OP** direction, the copolymer molecule varies from a star-shaped molecule to a linear one, changing the basic architecture of the

molecule, resulting in more dramatic morphology changes.

B. Two Grafts with Unequal Lengths ($f_B = 0.20$, $f_C = 0.40$). The triangle phase diagram of π-shaped ABC block copolymers with unequal graft lengths ($f_A = 0.40$, $f_B = 0.20$, and $f_C = 0.40$) is given in Figure 3. There is no reflection symmetry in Figure 3 with respect to the vertical line where $f_{A1}/f_A = 0.50$.

At point **P** in Figure 3, where the volume fractions of A1 and A3 are zero and the volume fraction of A2 is 0.40, the π-shaped block copolymer becomes a linear triblock copolymer and the LAM3 morphology is found, which is the same as that reported in ref 8. Near point **P**, where the volume fractions of A1 and A3 are small and the volume fraction of A2 is large, only one type of morphology (LAM3) is found. This is in agreement with
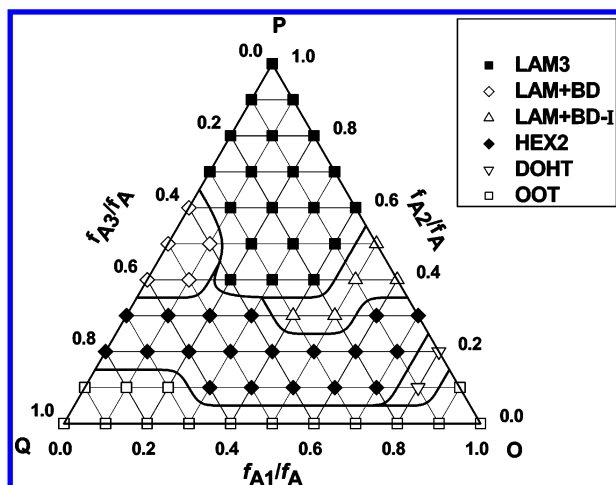
Figure 3. Phase diagram for $f_A = 0.40$ and $f_B = 0.20$, $f_C = 0.40$, and $\chi_{AB}N = \chi_{AC}N = \chi_{BC}N = 50$. The solid lines are shown to guide the eye.

ref 8 for the linear BAC triblock copolymer at the same volume fractions. As the volume fractions of A1 and A3 decrease and the volume fraction of A2 increases, the π-shaped block copolymer is close to linear BAC triblock copolymer, where A is the middle block.

Now we focus on the **OQ** edge in Figure 3. At point **O** and point **Q** the architectures of the two block copolymers are the same (three-arm block copolymer), and the OOT morphology is observed. This is in agreement with ref 9 at the same composition. Along the **OQ** edge, the architecture of the block copolymer changes from three-arm to four-arm and finally back to three-arm block copolymer again, and only the OOT morphology is found. Near the **OQ** edge, the trend is similar to that in Figure 2. When fixing $f_{A2}/f_A = 0.20$, we find the HEX2 morphology except at the point of $f_{A1}/f_A = 0.8$, where the A-rich domain is continuous and C-rich domains are hexagonal, and there are six B-rich hexagons around each C-rich domain, which is different from the hexagonal lattice phase (HEX) or the core−shell hexagonal lattice phase (CSH) reported in refs 8 and 9. At $f_{A1}/f_A = 0.8$ on the **OP** edge, the DOHT morphology is observed, which also has been found in ref 24 with symmetric interactions.

Along the **QP** edge we fix the B block at one end of A and move the C block to the other end, whereas along the **OP** edge, we fix the C block at one end of A and move the B block to the other end. Note that we have different B and C lengths. Thus, we find, along the **OP** edge in Figure 3 the ordered microphases change from OOT, to DOHT, to HEX2, to LAM + BD-I, and finally to LAM3. However, along the **QP** edge in Figure 3 the ordered microphases change from OOT, to HEX2, to LAM + BD, and finally to LAM3. It is also found that along the **OP** edge the LAM3 appears earlier than along the **QP** edge. This can be attributed to the particular molecular architecture of the π-shaped block copolymer, in which the volume fraction of the C block is larger than that of the B block. Furthermore, when the volume fraction of A3 is fixed, the larger the volume fraction of the B block, the less influence of the A3 on the phase behavior. Near the **OP** edge in Figure 3, we find similar transitions.

Summary

Using a combinatorial screening method based on the SCFT for polymers, we have investigated the morphol-

ogies of a π-shaped ABC block copolymer, in which A is the backbone and B and C are the two grafts. In this work, the order−order transitions for copolymers of different architectures ranging from star block copolymer to linear triblock copolymer are discussed. By systematically varying the positions of graft points B and C, namely by changing the volume fractions of A1, A2, and A3, the triangle phase diagrams of the π-shaped ABC block copolymer with equal interactions among the three species are constructed. It is found that when the volume fractions of block B and block C are equal, the triangle phase diagram shows a reflection symmetry; When we fix the shorter block at one end of the backbone and move the longer block toward the other end along the backbone, the resulting morphology reaches the same as that of a linear triblock copolymer rapidly. These results may help the design and the synthesis of block copolymers with different microstructures.

References and Notes

(1) Milner, S. T. *Macromolecules* **1994**, *27*, 2333.
(2) Bates, F. S.; Fredrickson, G. H. *Phys. Today* **1999**, *52*, 32.
(3) Lee, C.; Gido, S. P.; Poulos, Y.; Hadjichristidis, N.; Tan, N. B.; Trevino, S. F.; Mays, J. W. *Polymer* **1998**, *39*, 4631.
(4) Lee, C.; Gido, S. P.; Poulos, Y.; Hadjichristidis, N.; Tan, N. B.; Trevino, S. F.; Mays, J. W. *J. Chem. Phys.* **1997**, *107*, 6460.
(5) Zhu, Y. Q.; Weidisch, R.; Gido, S. P.; Velis, G.; Hadjichristidis, N. *Macromolecules* **2002**, *35*, 5903.
(6) Turner, C. M.; Sheller, N. B.; Foster, M. D.; Lee, B.; Corona-Galvan, S.; Quirk, T. P. *Macromolecules* **1998**, *31*, 4372.
(7) Lee, C.; Gido, S. P.; Pitsikalis, M.; Mays, J. W.; Tan, N. B.; Trevino, S. F.; Hadjichristidis, N. *Macromolecules* **1997**, *30*, 3732.
(8) Tang, P.; Qiu, F.; Zhang, H. D.; Yang, Y. L. *Phys. Rev. E* **2004**, *69*, 031803.
(9) Tang, P.; Qiu, F.; Zhang, H. D.; Yang, Y. L. *J. Phys. Chem. B* **2004**, *108*, 8434.
(10) Helfand, E.; Wasserman, Z. R. *Macromolecules* **1976**, *9*, 879.
(11) Helfand, E.; Wasserman, Z. R. *Macromolecules* **1978**, *11*, 960.
(12) Helfand, E.; Wasserman, Z. R. *Macromolecules* **1980**, *13*, 994.
(13) Noolandi, J.; Hong, K. M. *Ferroelectrics* **1980**, *30*, 117.
(14) Hong, K. M.; Noolandi, J. *Macromolecules* **1981**, *14*, 727.
(15) Whitmore, M. D.; Noolandi, J. *J. Chem. Phys.* **1990**, *93*, 2946.
(16) Matsen, M. W.; Schick, M. *Phys. Rev. Lett.* **1994**, *72*, 2660.
(17) Matsen, M. W.; Schick, M. *Macromolecules* **1994**, *27*, 6761.
(18) Matsen, M. W.; Schick, M. *Macromolecules* **1994**, *27*, 7157.
(19) Matsen, M. W.; Bates, F. S. *Macromolecules* **1996**, *29*, 1091.
(20) Drolet, F.; Fredrickson, G. H. *Phys. Rev. Lett.* **1999**, *83*, 4317.
(21) Drolet, F.; Fredrickson, G. H. *Macromolecules* **2001**, *34*, 5317.
(22) Fredrickson, G. H.; Ganesan, V.; Drolet, F. *Macromolecules* **2002**, *35*, 16.
(23) He, X. H.; Liang, H. J.; Huang, L.; Pan, C. Y. *J. Phys. Chem. B* **2004**, *108*, 1731.
(24) Gemma, T.; Hatano, A.; Dotera, T. *Macromolecules* **2002**, *35*, 3225.

MA051303M